JPEDAV (2006) 27:659-664
DOI: 10.1361/154770306X153701
1547-7037/$19.00 ©ASM International

Interdiffusion Analysis for NiAl versus Superalloys Diffusion Couples

E. Perez, T. Patterson, and Y. Sohn

(Submitted March 23, 2006; in revised form July 17, 2006)

Solid-to-solid diffusion couples, β-NiAl (*B*2) versus various commercial superalloys (i.e., CM247, GTD-111, IN-939, IN-718, and Waspalloy) were examined to quantify the rate of Al interdiffusion as a function of initial superalloy composition. The diffusion couples were assembled with Invar steel jig encapsulated in Ar by sealing in quartz capsules and annealed at 1050 °C for 96 h. Concentration profiles measured by electron probe microanalysis in the single-phase β-NiAl region were used to determine interdiffusion fluxes and effective interdiffusion coefficients of individual components in the single-phase β-NiAl side of the couple. The values determined using experimental concentration profiles of the single-phase β-NiAl side of the couple were used to predict effective interdiffusion coefficients in multiphase superalloy side of the couple based on mass balance and local continuity of interdiffusion fluxes. Microstructural and compositional stability of protective coatings (e.g., NiCoCrAlY and NiAl) as a function of superalloys composition are discussed based on effective interdiffusion coefficients predicted from diffusion couple studies.

Keywords coatings, diffusion coefficients, interdiffusion, multicomponent, multiphase, superalloys

1. Introduction

Although Ni-base superalloys have excellent strength and creep resistance, they normally require protective coatings (i.e., oxidation resistance or thermal barrier coatings, TBCs, with bond coats) to meet the high-temperature demand of higher-performance turbine engines.[1] Typically, MCrAlY (where M = Ni and/or Co) with two-phase (i.e., Al rich, *B*2 β phase and Ni-rich face-centered cubic, or fcc, γ-phase) or single-phase β alloys are used as stand-alone oxidation resistance coatings or as bond coats in TBCs. In both MCrAlY and NiAl-based coatings, Al-rich β phase serves as an Al reservoir for the formation of continuous, stable, and protective Al_2O_3 scale.[1-7] During high-temperature exposure, Al-rich β phase gets dissolved due to depletion of Al from the coating. The loss of Al occurs by interdiffusion toward the surface of the coating to form Al_2O_3 and by interdiffusion with the superalloy. Several studies have shown that the interdiffusion between the coating and the superalloy substrate may contribute more to the overall Al depletion,[8-19] rather than the Al depletion caused by oxidation, although repeated spallation of the Al_2O_3 scale may accelerate the loss caused by oxidation. In general, when the Al concentration in the coating falls below about 10 at.%, after complete dissolution of the β phase, these coatings can no longer maintain the continuity of the scales and are considered no longer effective.

Commercial superalloys have been developed with compositions and heat treatments to optimize high-temperature strength, as well as resistance against creep, fatigue, oxidation, and hot corrosion. Also, and somewhat in parallel, similar optimizations of the composition for MCrAlY and NiAl-based coatings have been carried out to increase oxidation and hot-corrosion resistance. Considering the significance of diffusional interactions[20-24] in multicomponent alloys, the lifetime of the coatings, defined by depletion of Al, may be enhanced by controlling the interdiffusion fluxes of individual components, particularly for Al. Therefore, while a coating may be selected/designed for environmental degradation resistance, and a superalloy can be selected/developed based on strength and creep and fatigue resistances, a system selection/development should be optimized to control the interdiffusion fluxes of diffusing components, so that Al interdiffusion flux across the coating/superalloy interface is minimized.

In this study, diffusion couples consisting of single-phase *B*2 β-NiAl versus various commercial superalloys were examined. The measurement of concentration profiles (and thus interdiffusion fluxes and coefficients) by electron probe microanalysis (EPMA) is difficult for fine two-phase microstructures like that of the γ + γ′ in Ni-base superalloys. Therefore, in this study, quantitative determination of interdiffusion fluxes and coefficients were first carried out from concentration profiles measured in single-phase

This article was presented at the Multicomponent-Multiphase Diffusion Symposium in Honor of Mysore A. Dayananda, which was held during TMS 2006, 135th Annual Meeting and Exhibition, March 12-16, 2006, in San Antonio, TX. The symposium was organized by Yongho Sohn of University of Central Florida, Carelyn E. Campbell of National Institute of Standards and Technology, Richard D. Sisson, Jr., of Worcester Polytechnic Institute, and John E. Morral of Ohio State University.

E. Perez, T. Patterson, and **Y. Sohn,** Advanced Materials Processing and Analysis Center and Department of Mechanical, Materials and Aerospace Engineering, University of Central Florida. Contact e-mail: ysohn@mail.ucf.edu.

β-NiAl side of the couple. Then utilizing the general expression of average effective interdiffusion coefficient, along with mass balance and local continuity of interdiffusion flux, accumulated interdiffusion fluxes (e.g., integrated interdiffusion coefficients) and effective interdiffusion coefficients of individual components in superalloys were predicted. The predicted values were then examined as a function of nominal composition of various superalloys.

2. Interdiffusion Analysis

Interdiffusion flux of a component i in a multicomponent system can be defined as:[25-28]

$$\tilde{J}_i = -\sum_{j=1}^{n-1} \tilde{D}_{ij}^{n} \frac{\partial C_j}{\partial x} \qquad (i = 1, 2, \ldots, n-1) \qquad \text{(Eq 1)}$$

where $\tilde{J}_i$ is the interdiffusion flux of component i, $\tilde{D}_{ij}^{n}$ is the interdiffusion coefficient of component i with respect to the concentration gradient of j in an n component system, and $\partial C_j/\partial x$ is the $(n-1)$ independent concentration gradient. This method requires knowledge of $(n-1)$ independent concentration gradients and $(n-1)^2$ interdiffusion coefficients where n is the number of components in the system. This method becomes impractical for superalloy coating systems that normally contain eight or more components with at least, γ + γ′, and β + γ two-phase microstructures.

The interdiffusion fluxes of individual components may be determined directly from their concentration profiles without the need of the interdiffusion coefficients by:[25]

$$\tilde{J}_i = \frac{1}{2t} \int_{C_i^{\pm\infty}}^{C_i(x)} (x - x_o)\, dC_i \qquad (i = 1, 2, \ldots, n) \qquad \text{(Eq 2)}$$

where t is the diffusion anneal time. The profile of interdiffusion flux for a component can be integrated with respect to distance, and this accumulated interdiffusion flux for a component can be defined as integrated interdiffusion $\tilde{D}_i^{\text{int}}$ coefficients over a selected region, x_1 from x_2, as:

$$\tilde{D}_{i,\Delta x}^{\text{int}} = \int_{x_1}^{x_2} J_i\, dx \qquad \text{(Eq 3)}$$

An effective interdiffusion coefficient, $\tilde{D}_i^{\text{eff}}$, is then defined as:

$$\tilde{D}_{i,\Delta x}^{\text{eff}} = \frac{\tilde{D}_{i,\Delta x}^{\text{int}}}{C_i^{x_2} - C_i^{x_1}} \qquad \text{(Eq 4)}$$

This effective interdiffusion coefficient incorporates all multicomponent diffusional interactions for the system to provide an effective value for the interdiffusion of a component species as defined by:

$$\tilde{D}_i^{\text{eff}} = \tilde{D}_{ij}^{n} + \sum_j \frac{\tilde{D}_{ij}^{n}\, \partial C_j/\partial x}{\partial C_i/\partial x} \qquad (j \neq i) \qquad \text{(Eq 5)}$$

Since $\tilde{J}_i$ must be continuous at any location such as the Matano plane and the effective interdiffusion coefficient can be defined on either side of any location such as the Matano plane, (e.g., $\tilde{D}_{i,\text{L}}^{\text{eff}}$ and $\tilde{D}_{i,\text{R}}^{\text{eff}}$ for the left- and right-hand side of the Matano plane), the following relations can be defined:[26,27]

$$\tilde{J}_i|_{x=x_o} = \frac{\sqrt{\tilde{D}_{i,\text{L}}^{\text{eff}}}}{\alpha_{i,\text{L}}\sqrt{t}} (C_i^{-\infty} - C_i^{o}) = \frac{\sqrt{\tilde{D}_{i,\text{R}}^{\text{eff}}}}{\alpha_{i,\text{R}}\sqrt{t}} (C_i^{o} - C_i^{+\infty}) \qquad \text{(Eq 6)}$$

where $\alpha_{i,\text{L}}$ and $\alpha_{i,\text{R}}$ are dimensionless parameters. Based on the experimental concentration profile on one side of the Matano plane, Eq 6 can be used to predict the effective interdiffusion coefficient on the other side of the Matano interface provided that α_i does not deviate from $\sqrt{\pi}$.[26,27] This would be a good assumption for the concentration profile of an intrinsically fast-diffusing component such as Al. A similar equation for $\tilde{D}_i^{\text{int}}$ by substituting Eq 4 into Eq 6 can be defined as:

$$\frac{\tilde{D}_{i,\text{R}}^{\text{int}}}{\tilde{D}_{i,\text{L}}^{\text{int}}} = \left(\frac{C_i^{-} - C_i^{o}}{C_i^{o} - C_i^{+}} \right) \qquad \text{(Eq 7)}$$

Table 1 Composition of superalloys, CM-247, GTD-111, IN-738, IN-939, and Waspalloy measured by electron microprobe analysis using pure standards

Element, at.%	CM-247	GTD-111	IN-738	IN-939	Waspalloy
Al	14.20	6.80	7.24	4.45	3.16
Co	9.94	9.50	9.36	18.59	12.82
Cr	7.31	16.60	19.11	25.29	21.03
Fe	…	…	…	…	1.36
Mo	0.42	0.97	0.97	…	2.39
Nb	…	…	0.33	0.43	…
Ni	62.11	59.01	57.89	46.28	55.32
Ta	2.73	0.89	0.49	0.37	…
Ti	1.56	6.24	3.77	4.07	3.93
W	1.74	0.97	0.83	0.51	…
B(a)	0.82	…	…	0.05	…
C(a)	0.35	0.48	0.82	0.71	0.29
Hf(a)	…	…	0.5	…	…
Zr(a)	0.01	…	…	0.06	…

(a) Concentrations of trace elements are below detectable limit of electron probe microanalysis; therefore, they were obtained from the literature.

3. Experimental Procedure

Diffusion couples were assembled using hot-extruded β phase NiAl and several commercial superalloys, namely CM247 (Cannon-Muskegon Corporation, Muskegon, MI), GTD111 (General Electrical Company, Greenville, SC), IN738 (Special Metals Corporation, Huntington, WV), IN939 (Special Metals Corporation, Huntington, WV), and Waspalloy (Pratt & Whitney, East Hartford, CT). The average composition of these superalloys was measured using an electron probe microanalysis (EPMA), JEOL 733 Super-Probe (Tokyo, Japan), using pure standards and large (~100 μm) probe diameter. Table 1 reports the measured superal-

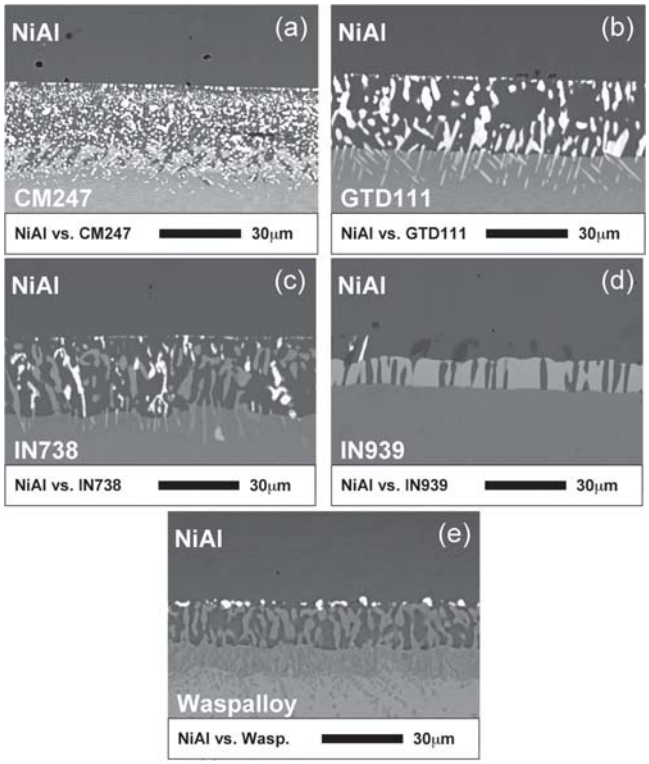

Fig. 1 Backscatter electron micrographs of diffusion microstructure observed in solid-to-solid diffusion couples, NiAl versus (a) CM-247, (b) GTD-111, (c) IN-738, (d) IN-939, and (e) Waspalloy, annealed at 1050 °C for 96 h

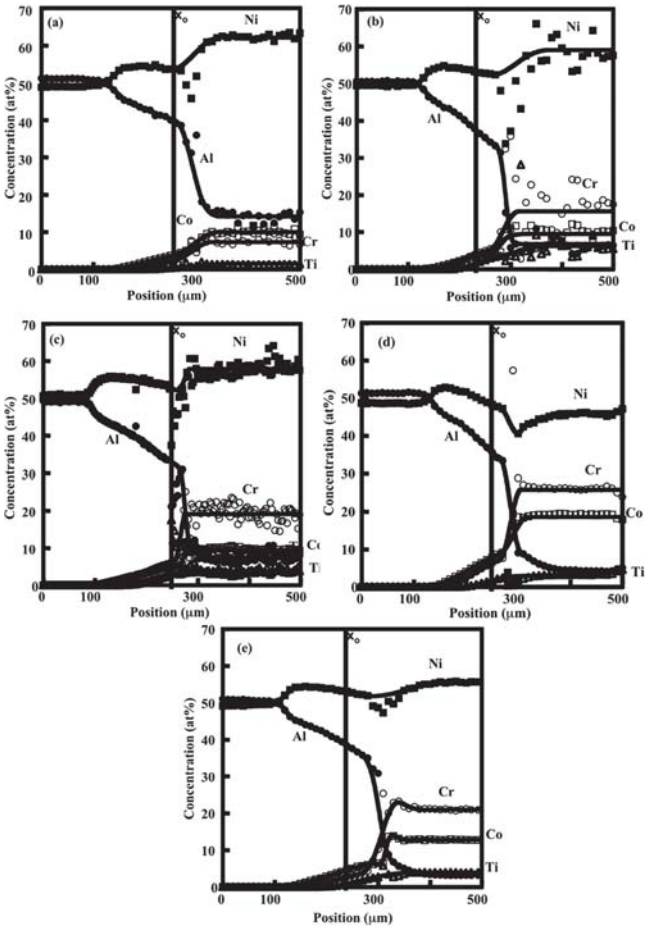

Fig. 2 Concentration profiles of major component in solid-to-solid diffusion couples, NiAl versus (a) CM-247, (b) GTD-111, (c) IN-738, (d) IN-939, and (e) Waspalloy, annealed at 1050 °C for 96 h. These profiles were determined by electron probe microanalysis using pure standards.

loy compositions. The trace elements present in the superalloys could not be precisely measured because their concentrations fall under the EPMA detection limits. The values presented for these components were obtained from the literature. Finally the compositions reported in Table 1 were balanced by Ni concentrations, and were near to those reported in literature. The β NiAl used for all diffusion couples was of near-stoichiometric composition with approximate equiaxed grain diameter of 30 to ~50 μm.

The NiAl and superalloys were prepared into disks approximately 8 mm in diameter by 3 mm in thickness. Surfaces were metallographically polished down to ¼ μm on a Stuers Rotopol (Westlake, OH) polisher using diamond paste. The polished surfaces were placed in contact with each other and were held together by two clamping disks with rods made of Invar steel. The couples were then placed in quartz capsules, sealed on one end, evacuated to 1×10^{-6} torr, and flushed with ultrahigh-purity hydrogen. The evacuation and hydrogen-flush was repeated several times, and the capsule was finally filled with ultrahigh purity argon. The final argon pressure in the capsule was controlled so that the pressure inside the capsule was approximately 1 atm at 1050 °C. The capsule was then sealed and placed at the center of a Lindberg/Blue (Asheville, NC) three-zone tube furnace. The furnace was then heated to 1050 °C within an hour. The furnace ends were fully insulated to minimize temperature gradients. The diffusion couples were annealed at 1050 °C isothermally for 96 h, and quenched in water by breaking the quartz capsule. The samples were then mounted in epoxy, cross sectioned, and metallographically polished with diamond paste down to ¼ μm. Microstructural analysis of the diffusion couples was carried out by backscatter electron imaging, and the concentration profiles within the diffusion couples were determined by EPMA using the JEOL 733 SuperProbe. Pure elemental standards were used for EPMA, and the data were collected at an accelerating voltage of 20 keV using a point-to-point technique.

4. Results and Discussion

Backscatter electron micrographs of diffusion couples, NiAl versus CM247, GTD111, IN738, IN939, and Waspalloy are shown in Fig. 1. Excellent diffusion bonding was achieved for each couple. Many small precipitates, such as TCP phases rich in refractory, were observed near the interface between NiAl and superalloys. These precipitates also prevent any meaningful determination of concentration profiles by EPMA in these zones and subsequent analysis.

The concentration profiles of the major elements ob-

Table 2 Integrated and effective interdiffusion coefficients of major constituents, Al, Co, Cr, Ni, Ti, determined from experimental concentration profiles on the NiAl side of the diffusion couples

Superalloy	Constituent element	$\tilde{D}^{int}_{NiAl}$	$\tilde{D}^{eff}_{NiAl}$	$\tilde{D}^{int}_{SA}$	$\tilde{D}^{eff}_{SA}$	$\tilde{D}^{int}_{Tot}$	$\tilde{D}^{eff}_{Tot}$
CM-247	Al	1.51	13.55	0.66	2.56	2.17	5.87
	Co	–0.25	6.46	–0.15	2.51	–0.40	4.02
	Cr	–0.09	3.73	–0.04	0.79	–0.13	1.78
	Ni	–1.56	32.7	–0.81	8.90	–2.37	17.74
	Ti	–0.006	1.34	–0.002	0.19	–0.008	0.51
GTD-111	Al	1.50	9.87	0.80	2.80	2.30	5.30
	Co	–0.25	6.06	–0.20	3.63	–0.45	4.74
	Cr	–0.21	4.40	–0.10	0.89	–0.31	1.87
	Ni	–0.99	31.37	–0.49	7.69	–1.48	16.02
	Ti	–0.04	1.49	–0.02	0.64	–0.06	0.96
IN-738	Al	1.91	12.72	1.06	3.90	2.97	6.92
	Co	–0.35	7.76	–0.31	6.41	–0.66	7.05
	Cr	–0.28	5.24	–0.11	0.76	–0.39	2.04
	Ni	–2.06	65.13	–0.16	38.01	–2.22	27.34
	Ti	–0.035	1.73	–0.041	2.35	–0.08	2.02
IN-939	Al	1.56	9.56	0.84	2.74	2.40	5.14
	Co	–0.52	6.37	–0.41	3.95	–0.93	5.00
	Cr	–0.28	4.26	–0.10	0.52	–0.38	1.50
	Ni	–0.73	–132.84	–0.22	–12.38	0.94	–38.46
	Ti	–0.03	1.49	–0.02	1.11	–0.05	1.23
Waspalloy	Al	2.34	16.16	1.02	3.10	3.36	7.15
	Co	–0.55	9.68	–0.44	6.24	–0.99	7.72
	Cr	–0.23	6.16	–0.05	0.28	–0.28	1.33
	Ni	–1.48	52.57	–1.30	40.61	–2.78	50.09
	Ti	–0.04	2.04	–0.03	1.25	–0.07	1.78

Note: All interdiffusion coefficients, $\tilde{D}^{int}$ and $\tilde{D}^{eff}$ are reported in 10^{-15} m^2/s.
The integrated and interdiffusion coefficients for the superalloy side of the diffusion couples were predicted based on Eq 6 and 7.

tained from the diffusion couples of NiAl versus CM247, GTD111, IN738, IN939, and Waspalloy are shown in Fig. 2. In these profiles, as expected, concentrations determined on the single-phase β NiAl side are consistent without any scatter, while those on the multiphase superalloy side, including the precipitates near the interface exhibit large scatter. This scattering in concentrations due to multiphase regions does not allow any meaningful and quantitative analysis of interdiffusion. However, it should be noted that the concentration profiles determined by EPMA was smoothened, after excluding obvious scatters, for the approximate determination of Matano plane for the simplicity of presentation and discussion, although the analysis of interdiffusion presented in this work can be applied to any plane (i.e., location) within the diffusion zone.

Integrated, $\tilde{D}^{int}_{i,NiAl}$, and effective, $\tilde{D}^{eff}_{i,NiAl}$, interdiffusion coefficients for the NiAl side of the diffusion couples were calculated using Eq 3 and 4 and are reported in Table 2. Then, Eq 6 and 7 were used to predict $\tilde{D}^{int}_{i,SA}$ and $\tilde{D}^{eff}_{i,SA}$ for the superalloy side of the couples as reported in Table 2. The terminal compositions required for these predictions were obtained from Table 1 for the superalloys and from EPMA measurements for the NiAl in each couple.

In Table 2, all $\tilde{D}^{int}_{i,NiAl}$ and $\tilde{D}^{eff}_{i,NiAl}$ are greater for the NiAl side of the diffusion couples, except in the case of the IN738 couple, where $\tilde{D}^{int}_{Ti,SA}$ and $\tilde{D}^{eff}_{Ti,SA}$ are slightly higher in magnitude than $\tilde{D}^{int}_{Ti,NiAl}$ and $\tilde{D}^{eff}_{Ti,NiAl}$. In the case of the IN939 diffusion couple, $\tilde{D}^{eff}_{Ni,NiAl}$ and $\tilde{D}^{eff}_{Ni,SA}$ are negative, and this indicates that cross-interdiffusion coefficients are appreciable. The $\tilde{D}^{int}_{i,total}$ provided in Table 2 is a measure of the integrated interdiffusion flux of individual components in diffusion couples. The $\tilde{D}^{eff}_{i,total}$ in Table 2 is an average effective interdiffusion coefficient of individual components in the diffusion couples. The calculated and predicted values can be used to design and/or select appropriate compositions of coatings and/or superalloys to minimize degradation due to interdiffusion.

To validate $\tilde{D}^{eff}_{i,SA}$ predicted for the superalloy side from the β NiAl side of the diffusion couples, the full concentration profiles of the CM247 superalloy, which contained minimal scatter, were analyzed to estimate $\tilde{D}^{eff}_{i,SA}$ for each component directly from the concentration profile. The magnitudes of $\tilde{D}^{eff}_{i,SA}$ predicted from Eq 6 were within 10% of those determined by using the experimental concentration profiles of CM247. It should be noted that the concentration profiles of CM247 are exceptionally consistent, and that the same analysis cannot be carried out for other superalloys with significant scatter in concentration profiles.

Predicted $\tilde{D}^{eff}_{Al,SA}$ were examined as a function of initial superalloy compositions. In general, superalloys with higher concentration of Cr, Mo, and Ti had higher $\tilde{D}^{eff}_{Al,SA}$. Higher concentrations of Ta, W, and Al in the superalloys were related to lower $\tilde{D}^{eff}_{Al,SA}$. While this is not a direct indication of diffusional interaction (e.g., cross terms), additional experiments with simplified diffusion couples may be carried out to determine each of the components direct interactions with Al.

Fleetwood[12] previously identified the fact that higher concentrations of refractory elements promote the formation of precipitate phases that develop in the interdiffusion zone and effectively reduce the cross-sectional area for interdiffusion. Compositions reported in Table 1 and image analyses indicate that while higher concentrations of refractory element promote the formation of precipitates, they do not necessarily lead to a reduction of the cross-sectional area for interdiffusion due to morphological variations.[12] Higher concentrations of refractory elements in general were found to reduce the effective interdiffusion coefficients for Al by means of multicomponent diffusional interactions.

5. Summary

Interdiffusion of Al into selected Ni-base superalloys was examined using diffusion couples NiAl versus CM247, GTD111, IN738, IN939, and Waspalloy. The concentration profiles obtained by EPMA on the single-phase NiAl side of the couple were analyzed for the determination of integrated and effective interdiffusion coefficients for the NiAl side of the couple. Based on mass-balance and continuity of interdiffusion flux, the values determined for NiAl side of the couple were used to predict the integrated and effective interdiffusion coefficients for the multiphase superalloy side of the diffusion couple (i.e., fine $\gamma + \gamma'$ microstructure with refractory-rich precipitates). In general, superalloys with higher concentration of Cr, Mo, and Ti yielded higher $\tilde{D}^{eff}_{Al,SA}$, while higher concentrations of Ta, W, and Al in the superalloys were related to lower $\tilde{D}^{eff}_{Al,SA}$.

Acknowledgments

This work was financially supported by National Science Foundation CAREER award (DMR-0238356) with additional support from U.S. DOE's University Turbine Systems Research Fellowship administered by Clemson University, and Undergraduate Research Initiative of University of Central Florida. The authors also acknowledge technical assistance and discussion with Mr. P. Anderson at Exxon-Mobil, Mr. A. Burns at Siemens Power Generation, and Dr. Richard Krutenat. This manuscript is based on the M.S. thesis submitted by Mr. Emmanuel Perez.

References

1. K. Hünecke, *Jet Engines,* Motorbooks Int. 1997, 6th print, 2003
2. C.T. Simms, N.S. Stoloff, and W.C. Hagel, *Superalloys II,* John Wiley & Sons, 1987
3. M.J. Donachie and S.J. Donachie, *Superalloys: A Technical Guide,* 2nd ed., ASM International, 2002
4. J.A. Nesbitt and R.W. Heckel, Modeling Degradation and Failure of Ni-Cr-Al Overlay Coatings, *Thin Solid Films,* 1984, **119,** p 281-290
5. J.A. Nesbitt, E.J. Vinarcik, C.A. Barret, and J. Doychak, Diffusional Transport and Predicting Oxidative Failure During Cyclic Oxidation of β-NiAl Alloys, *Mater. Sci. Eng. A,* 1992, **A153,** p 561-566
6. J.A. Nesbitt and R.W. Heckel, Diffusional Transport During the Cyclic Oxidation of $\gamma + \beta$, Ni-Cr-Al (Y,Zr) Alloys, *Oxid. Met.,* 1988, **29,** p 75-102
7. N.S. Cheruvu, K.S. Chan, and G.R. Leverant, "Coating Life Prediction for Combustion Turbine Blades," International Gas Turbine & Aeroengine Congress & Exhibition (Stockholm, Sweden), June 2-5, 1998, 98-GT-478
8. E.Y. Lee, D.M. Charter, R.R. Biederman, and R.D. Sisson Jr., Modeling the Microstructural Evolution and Degradation of M-Cr-Al-Y Coatings During High Temperature Oxidation, *Surf. Coat. Technol.,* 1987, **32,** p 19-39
9. M.S. Thompson and J.E. Morral, Kinetics of Coating/Substrate Interdiffusion in Multicomponent Systems, *High Temperature Coatings: Proc. Symposium on High Temperature Coatings,* M. Khobaib and R.C. Krutenat, Ed., Metallurgical Society, 1986, p 55-66
10. K.L. Luthra and M.R. Jackson, Coating/Substrate Interactions at High Temperature, *High Temperature Coatings: Proc. Symposium on High Temperature Coatings,* M. Khobaib and R.C. Krutenat, Ed., Metallurgical Society, 1986, p 85-100
11. J.E. Morral, Interdiffusion and Coating Design, *Surf. Coat. Technol.,* 1990, **43/44,** p 371-380
12. M.J. Fleetwood, Influence of Nickel-Base Alloy Composition on the Behavior of Protective Aluminide Coatings, *J. Inst. Met.,* 1970, **98,** p 1-7
13. M.A. Dayananda, Multicomponent Diffusion Studies in Selected High Temperature Alloy Systems, *Mater. Sci. Eng. A,* 1989, **A121,** p 351-359
14. C.W. Yeung, W.D. Hopfe, J.E. Morral, and A.D. Romig Jr., Interdiffusion in High Temperature Two Phase Ni-Cr-Al Coating Alloys, *Mater. Sci. Forum,* 1994, **163-165,** p 189-194
15. J.E. Morral and R.H. Barkalow, Analysis of Coating/Substrate Interdiffusion with Normalized Distance and Time, *Scr. Metall.,* 1982, **16,** p 593-594
16. K.A. Ellison, J.A. Daleo, and D.H. Boone, Interdiffusion Behavior in NiCoCrAlYRe-Coated IN-738 at 940° and 1050 °C, *Superalloys 2000, Proc. Ninth International Symposium on Superalloys* (Seven Springs, PA), Sept 17-21, 2000, T.M. Pollock et al., Ed., p 649
17. B. Wang, R.F. Huang, G.H. Song, J. Gong, C. Sun, L.S. Wen, and Y.F. Han, Interdiffusion Behavior of Ni-Cr-Al-Y Coatings Deposited by Arc-Ion Plating, *Oxid. Met.,* 2001, **56,** p 1-13
18. B. Wang, J. Gong, C. Sun, R.F. Huang, and L.S. Wen, The Behavior of MCrAlY Coatings on Ni_3Al-base Superalloy, *Mater. Sci. Eng. A,* 2003, **A357,** p 39-44
19. B. Gleeson, E. Basuki, and A. Crosky, Interdiffusion Behavior of an Aluminide Coated Nickel-Base Alloy at 1150 °C, *Elevated Temperature Coatings: Science and Technology IV,* N.B. Dahotre, J.M. Hampikian, and J.E. Morral, Ed., TMS, 2001, p 119-132
20. M.A. Dayananda, D.A. Behnke, and L.M. McCaslin, Interdiffusion and b-Phase Recession in MCrAlY Coatings on Selected Ni-Base Alloys, *Diffusion Analysis and Applications,* A.D. Romig, Jr. and M.A. Dayananda, Ed., TMS, 1989, p 325
21. Z. Mutasim, J. Kimmel, and W. Brentnall, "Effects of Alloy Composition on the Performance of Diffusion Aluminide

Coatings," International Gas Turbine & Aeroengine Congress & Exhibition (Stockholm, Sweden), June 2-5, 1998, 98-GT-401
22. H. Wei, X. Sun, Q. Zheng, G. Hou, H. Guan, and Z. Hu, An Inverse Method for Determination of the Interdiffusivity in Aluminide Coatings Formed on Superalloy, *Surf. Coat. Technol.,* 2004, **182,** p 112-116
23. Y.H. Sohn, E.Y. Lee, and R.D. Sisson Jr., Life Prediction and Life Extension of Thermal Barrier Coatings for Gas Turbine Engines, *Proc. 1992 Coatings for Advanced Heat Engine Workshop,* Sponsored by Office of Transportation Technology, Assistant Secretary for Conservation and Renewable Energy, U.S. Department of Energy, 1992, p II:49-60
24. K.S. Chan, N.S. Cheruvu, and G.R. Leverant, Predicting Coating Degradation under Variable Peak Temperature, *Proc. International Gas Turbine & Aeroengine Congress & Exhibition,* 1999
25. M.A. Dayananda and C.W. Kim, Zero-Flux Planes and Flux Reversals in Cu-Ni-Zn Diffusion Couples, *Metall. Trans. A,* 1979, **10A,** p 1333-1339
26. M.A. Dayananda and Y.H. Sohn, Average Effective Interdiffusion Coefficients and Their Applications for Isothermal Multicomponent Diffusion Couples, *Scr. Mater.,* 1996, **35,** p 683-688
27. M.A. Dayananda, Average Effective Interdiffusion Coefficients in Binary and Multicomponent Alloys, *Defect Diffus. Forum,* 1993, **95-98,** p 521-535
28. J. Crank, *The Mathematics of Diffusion,* 2nd ed, Oxford Science Publications, 1975